HHS Public Access

Author manuscript

ACS Appl Mater Interfaces. Author manuscript; available in PMC 2018 July 19.

Published in final edited form as:

ACS Appl Mater Interfaces. 2017 July 19; 9(28): 23409–23419. doi:10.1021/acsami.7b04932.

Anti-Cancer Therapeutic Alginate-Based Tissue Sealants for Lung Repair

Spencer L. Fenn[1,2], **Patrick N. Charron**[3], and **Rachael A. Oldinski**[2,3,4,5,*]

[1]Department of Biomedical Engineering, Tufts University, Medford, MA, 02155

[2]Bioengineering Program, College of Engineering and Mathematical Sciences, and Larner College of Medicine, University of Vermont, Burlington, VT, 05405

[3]Department of Mechanical Engineering, College of Engineering and Mathematical Sciences, University of Vermont, Burlington, VT, 05405

[4]Department of Electrical and Biomedical Engineering, College of Engineering and Mathematical Sciences, University of Vermont, Burlington, VT, 05405

[5]Department of Orthopaedics and Rehabilitation, Larner College of Medicine, University of Vermont, Burlington, VT, 05405

Abstract

Injury to the connective tissue that lines the lung, the pleura, or to the lung itself can occur from many causes including trauma or surgery, as well as lung diseases or cancers. To address current limitations for patching lung injuries, to stop air or fluid leaks, an adherent hydrogel sealant patch system was developed, based on methacrylated alginate (AMA) and AMA di-aldehyde (AMA-DA) blends, which is capable of sealing damaged tissues and sustaining physiological pressures. Methacrylation of alginate hydroxyl groups rendered the polysaccharide capable of photo-crosslinking when mixed with an eosin Y-based photo-initiator system, and exposed to visible green light. Oxidation of alginate yields functional aldehyde groups capable of imine bond formation with proteins found in many tissues. The alginate-based patch system was rigorously tested on a custom burst pressure testing device. Blending of non-oxidized material with oxidized (aldehyde modified) alginates yielded patches with improved burst pressure performance, and decreased delamination as compared with pure AMA. Human mesothelial cell (MeT-5A) viability and cytotoxicity were retained when cultured with the hydrogel patches. The release and bioactivity of doxorubicin-encapsulated sub-microspheres enabled the fabrication of drug-eluting adhesive patches, and were effective in decreasing human lung cancer cell (A549) viability.

TOC image

[*]**Contact/Corresponding Author:** Rachael A. Oldinski, 33 Colchester Ave, Burlington, VT 05405, oldinski@uvm.edu, 802-656-3338.

Author Contributions

The manuscript was written through contributions of all authors. All authors have given approval to the final version of the manuscript.

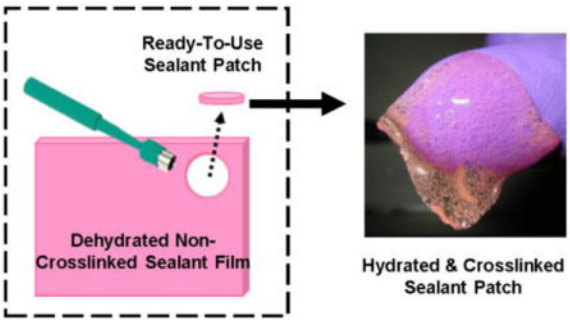

Keywords

Visible light crosslinking; alginate; aldehyde; burst pressure; tissue sealant; lung; drug delivery

1. INTRODUCTION

Lung leaks, due to damage in the pleural lining, or resected tissue, are a major medical problem associated with increased morbidity, mortality, and health care costs.[1–6] Trauma, or complications of pulmonary surgery, can result in air or liquid leaking out of the lung and into the pleural space, i.e., chest cavity, decreasing lung volume and causing the lung to collapse (pneumothorax), ultimately requiring emergent placement of a chest tube, an invasive approach associated with complication and limitations, to re-inflate the lung.[1–4, 7] Chronic pleural effusions related to underlying lung cancers, or cancers metastatic to lung (malignant effusions), are especially difficult to treat, apart from surgical interventions or pleurodesis. Physical pleurodesis is a surgical technique involving suturing, or pleural abrasion procedures, through the use of thoracotomy.[8] Chemical pleurodesis consists of applying a nocuous material, such as talc, on the lung surface to cultivate an inflammatory response.[9–10]

Few effective means exist of patching a lung injury to effectively stop an air or fluid leak and allow appropriate healing to occur. Although one photopolymerizable sealant, FocalSeal-L (Focal, Inc.) was previously investigated showing some success and gaining FDA approval in 2000, this product ultimately failed to enter the U.S. commercial market due to poor clinical performance.[11–12]In fact, there is currently only one surgical sealant approved for use as a lung tissue sealant, Progel™ (Bard-Davol), a polyethylene glycol-based product which utilizes human-derived serum albumin as a crosslinking agent.[13–15] The use of human-derived products not only increases cost but can also introduce immunogenic risk factors, and thus synthetic biomaterial sealants are sought to alleviate these concerns. Approaches using fibrin or cyanoacrylate glues or other liquid sealants, applied either directly to the lung surface or instilled into the airways have not been widely successful to date and have not been pursued further for use in these applications.[16–20] In addition, prolonged tissue damage due to an underlying disease, infection or cancer has not been addressed by the current methods. Indeed, surgical sealant tools are available to surgeons when closing or sealing surgical sites or wounds in tissue, yet due to the dynamic movement and stretch imposed on lung tissues, few have shown efficacy at physiological lung

pressures.[18, 21–22] Hydrogels are natural or synthetic-based crosslinked polymer networks that swell but do not dissolve in aqueous media, and the investigation of hydrogels to treat pulmonary and alveolar air leaks initiated in the late 1980's.[23]

Alginate and alginate-based hydrogels are investigated for biomedical applications due to their inherent non-toxicity, biocompatibility, and ready availability.[24] Derived from brown algae, alginate is desirable not only for those attributes already listed, but also for its relatively low cost and the various applications it can be used for drug delivery and tissue engineering.[25] Chemical modification of alginate has been studied extensively for improving upon the physical and mechanical properties of ionically crosslinked alginate gels.[26–28] Methacrylation of alginate imparts a functional group capable of light-activated covalent crosslinking (i.e. photo-crosslinking) by free radical polymerization in the presence of a photo-initiator.[24, 29–32] Alginate is inherently non-adhesive; however, oxidation of the backbone structure will elicit functional groups capable of forming crosslinks with extracellular matrix proteins, such as those found on the pleural surface.[33–36] Indeed, the incorporation of functional aldehyde groups has been investigated in several hydrogel biomaterial platforms for use in tissue engineering[37–53] and bio-adhesive applications.[35, 43, 54–57]

To address current limitations for patching lung injuries, to stop air or fluid leaks, an adherent hydrogel sealant patch system was developed, based on methacrylated alginate (AMA) and AMA di-aldehyde (AMA-DA) blends, which is capable of sealing damaged tissues and sustaining physiological pressures. The goal of this study was to develop a sealant that not only provides a reliable seal, but that can also control the release of soluble drugs to treat diseases, such as cancer. We illustrate the ability to control bioactive doxorubicin hydrochloride (DOX) release, one of the most widely used chemotherapeutic drugs, through micro-encapsulation techniques, and subsequent mixing with the polymer precursor solutions prior to tissue sealant patch fabrication.

2. MATERIALS AND METHODS

2.1. Synthesis of methacrylated alginate (AMA)

Methacrylated alginate (AMA) was synthesized as previously described.[24, 56] Briefly, a 2% (w/v) solution of Manugel® GMB (MW≈ 170–240 kDa, FMC Biopolymer) in deionized (DI) water was mixed with a 20-fold molar excess of methacrylic anhydride (Sigma-Aldrich). The solution was maintained at pH 8 using 5 N sodium hydroxide (Fisher) for 24 hours. Purification was performed via dialysis (MWCO=6–8 kDa) against DI water for 5-days, and lyophilized to yield a dry product. A 1% (w/v) AMA was prepared in deuterium oxide (D_2O, Acros Organics) and subsequently analyzed using ^{1}H-NMR spectroscopy (Bruker AVANCE III 500 MHz high-field NMR spectrometer), for 64 scans at 20 Hz. The degree of methacrylation (DOM) was established through integration of the peaks associated with methacrylate (6.24, 5.78 ppm) and alginate methyl resonances (1.96 ppm), and calculation of the ratios between.[29, 56, 58]

2.2. Synthesis of methacrylated alginate dialdehyde (AMA-DA)

To retain the ability to photo-crosslink while simultaneously improving the adhesive properties to tissue/proteins, AMA was oxidized to yield AMA dialdehyde (AMA-DA). A 1% AMA solution was prepared in DI water and reacted with sodium periodate (Sigma) at 0.25% (w/v) or 0.5% (w/v) to yield AMA-DA solutions with theoretical degrees of oxidation (DOO) of 25% (AMA-25DA) and 50% (AMA-50DA), respectively.[34–36, 43, 56] The products were dialyzed against DI water for 48 hours, and lyophilized to obtain dry AMA-DA. One percent (w/v) AMA-DA solutions were prepared in D_2O and subsequently analyzed using ^{1}H-NMR spectroscopy, for 64 scans at 20 Hz. The DOO was calculated by taking integrals of the alginate methyl protons at 5.0 ppm and the newly formed methyl protons at 5.17, 5.48 and 5.68 ppm, and subsequent comparison of ratios.[35–36]

2.3. Visible light crosslinking and gelation kinetics

AMA and AMA-DA solutions were analyzed using a rheometer (AR2000, TA Instruments) to determine if functionalization modulated the physical and mechanical properties of the molecules in solution or crosslinked as hydrogels. The viscosity and gelation kinetics of alginate (Alg), AMA, and AMA-DA precursor solutions and resulting hydrogels were determined. All tests were performed at 37°C using a 20-mm diameter 1°59′6″ steel cone geometry with a truncation gap of 57 μm; 6% (w/v) polymer solutions were prepared in phosphate buffered saline (PBS) with photo-initiators added at the following final concentrations:1 mM Eosin Y (photo-sensitizer, Acros Organics), 125 mM triethanolamine (initiator, Sigma), 20 mM 1-vinyl-2-pyrrolidinone (catalyst, Sigma).[59–61] Viscosity was measured at shear rates ranging from 1–100 (1/s), over a 60 second time period, using non-crosslinked precursor solutions. Gelation kinetics of the precursor solutions were assessed using an oscillatory time sweep at 10% radial strain and 1 Hz during exposure to visible green light [525 nm, custom 9.84 cm diameter light emitting diode (LED) array, NFLS-G30X3-WHT, SuperBrightLEDs] for 5 minutes. Shear storage moduli (G′)were calculated using analytical software (TA Data Analysis).

2.4. Hydrogel sealant patch fabrication

Lung sealant patches were fabricated using an injection molding technique. Polymer solutions (3% and 6% w/v) in DI water were prepared using AMA, AMA-25DA, AMA-50DA powders, and were subsequently blended at 1:1, or 1:2, weight ratios. Polymer solutions were then supplemented with photo-initiators as described in Section 2.3, and were protected from exposure to light. Precursor solutions were injected between two sheets of polytetrafluoroethylene (Teflon™) with a 1 mm spacer, using a syringe and 20-gauge needle, taking care to avoid the formation of air-bubbles (Figure 1A). The mold was then rapidly frozen using liquid nitrogen (vapor phase) and freeze-dried via lyophilization. Once dry, the mold was disassembled and the newly formed dry film of material was cut into individual patches using circular biopsy punches. It is important to note that at this stage, the patches have not yet undergone photo-crosslinking, yet contain photo-initiators required to induce photo-crosslinking once exposed to visible green light.

2.5. Burst pressure and failure analysis

To assess the performance of sealant patch formulations, ASTM F2392-04 was modified to build and utilize a custom-built burst pressure testing device, as previously described and depicted.[56, 62] Briefly, a polyether ether ketone device was designed to securely fasten a membrane/substrate across an open chamber, using a fluoroelastomer o-ring and clamp, which can be pressurized using an air-filled syringe and syringe pump (PHD 2000 Infuser, Harvard Apparatus). Collagen-rich substrates (Collagen Casings, The Sausage Maker Inc.) were used as an *in vitro* test membrane per the standard.[62] Substrates were hydrated in PBS at 37°C for at least 30 minutes prior to testing. Pressures within the chamber were recorded digitally using a USB-connected pressure transducer (Omega PX-409-030AUSBH) attached to the chamber through a side NPT-port. The entire apparatus was housed in an incubator held at 37°C. High-speed video (120 frames per second) was recorded during testing using a camera (Hero4, GoPro) with attached macro lens, which has been mounted within the incubator. Video was utilized to assess the mechanism of failure, either adhesive failure (delamination) or material failure (burst).[56]

To verify that each substrate was free from defects and leaks, the substrate was clamped down in the burst pressure device and pressurized with air to a baseline of 12 in H_2O, at an infusion rate of 75 mL/hr, and held briefly ensuring no change in pressure (i.e., no leaking occurred). Once substrate integrity was confirmed, the membrane was removed from the device and a small defect was created in the membrane using a 1.5 mm diameter biopsy punch (Figure 1B). Over these defects, 8 mm diameter sealant patches were applied to the membrane, and hydrated using 20 μL of PBS at 37°C (Figure 1C). The sealant was then photo-crosslinked for 5 minutes using a custom LED array (*vida supra*). Once cured, the now-sealed membrane was returned to the burst-pressure testing apparatus (Figure 1D), and pressurized with air at an infusion rate of 75 mL/hr until failure of the sealant was observed.

2.6. *In vitro* hydrolytic degradation

To determine if the sealant hydrogel was susceptible to hydrolytic degradation, the effects of degradation on hydrogel mass and swell ratios were quantified. Crosslinked hydrogels fabricated from 6% AMA:AMA-25DA at 1:1 ratio were first weighed (dry), and subsequently placed in cell culture media in a shaker-incubator at 37°C for 14-days. On days 1, 3, 7, and 14, samples were removed and weighed (wet), freeze-dried, then weighed (dry) to obtain both swell ratios and changes in mass.

2.7. Hydrogel sealant cytotoxicity

To assess the cytotoxicity of AMA and AMA-DA patches, MeT-5A human mesothelial cells (ATCC® CRL9444™) were cultured in the presence of photo-crosslinked sealant materials over a 24-hour period (n=3). Mesothelial cells were maintained at 37°C and 5% CO_2 in Medium 199 (Sigma) supplemented with the following components: 10% fetal bovine serum (FBS, Hyclone), 3.3 nM epidermal growth factor (EGF, Sigma), 400 nM hydrocortisone, 870 nM bovine insulin (Sigma), 20 mM HEPES (Sigma), 3.87 μg/L selenious acid (Aldrich), Trace Elements B Liquid used at 1,000 dilution (Corning). Cell viability, cytotoxicity and apoptosis were assessed using an ApoTox-Glo™ Triplex Assay (Promega Corporation) per the manufacturers protocol, and metabolic activity was assessed using an

thiazolyl blue tetrazolium bromide (MTT, Sigma) based assay. Cells were cultured in 24-well Transwell® plates, with each insert loaded with 10 mg AMA, AMA-25DA and AMA-50DA material which was hydrated and crosslinked prior to insertion into seeded (50,000 cells/well) plate wells.

After 24 hours of culture with test materials, the ApoTox-Glo™ viability/cytotoxicity reagent was prepared and added to each well per the manufacturers protocol allowed to culture at 37°C for an additional 30 minutes, then the plate was assessed using a plate reader (H1 Synergy, BioTek) to measure fluorescence intensity at the following excitation and emission wavelengths: $400_{Ex}/505_{Em}$ nm (viability) and $485_{Ex}/520_{Em}$ nm (cytotoxicity). Successively the apoptosis reagent was prepared, added to each well, and allowed to culture for an additional 30 minutes at room temperature, and the luminescence was quantified using the plate reader.

After 24 hours of culture with test materials, a previously prepared MTT-solution in PBS was added to each test well, up to a final concentration of 0.5 mg/mL, mixed briefly on an orbital shaker, and incubated at 37°C for 3 hours. Next, the cell culture media and excess MTT-solution were aspirated from each well and replaced with dimethyl sulfoxide (DMSO, Sigma) to solubilize the formazan crystals using gentle orbital shaking. Absorbance was assessed at 540 nm wavelength, the peak absorbance of formazan in DMSO, using a plate reader. Background absorbance was assessed at 690 nm wavelength and subtracted from the absorbance observed at 540 nm to obtain a corrected absorbance reading of cell mitochondrial activity.

2.8. Fabrication of DOX-loaded AMA sub-microspheres

Doxorubicin hydrochloride (DOX) was encapsulated within alginate sub-microspheres as described in a prior study.[29] Briefly, a 2% (w/v) AMA solution was prepared in DI water, and subsequently supplemented with 0.1% (w/v) DOX (Sigma).[29] Additionally, photo-initiators were added to the mixture, as listed in Section 2.3. DOX-encapsulated hydrogel sub-microspheres were formed using a water-in-oil emulsion technique and covalently photo-crosslinked using visible green light.[29, 63] At room temperature, DOX-loaded hydrogel precursor solution was added dropwise to bioreagent-grade mineral oil containing 5% (v/v) Span 80, consistently mixing at 1200 rpm for 5 minutes. Next, 30% (v/v) Tween 80 (in bioreagent-grade mineral oil) was added and mixed for a further 5 minutes. Emulsion droplets were photo-crosslinked for 5 minutes using visible green light produced by a custom LED-array.[29] Sub-microspheres were washed in isopropanol and DI water, and subsequently freeze-dried for storage. Sub-microsphere size was assessed by dynamic light scattering (DLS, Zetasizer Nano, Malvern), using a dilute suspension in PBS (pH 7.4) at 37°C. Encapsulation efficiency was assessed and calculated as described previously.[29]

2.9. Chemotherapeutic-loaded sealant

Hydrogel sealant precursor solutions were prepared as described in Section 2.4, using formulations for the two highest performing patches, 6% AMA:AMA-25DA and 6% AMA:AMA-50DA, blended at a 1:1 weight ratio. Polymer solutions were subsequently blended with 800 μg/mL DOX-encapsulated sub-microspheres. The solutions were quickly

injected into molds (see Section 2.4.), frozen, and lyophilized to form DOX-eluting sealant patches.

2.10 Chemotherapeutic drug release

To assess drug-release kinetics of the DOX-loaded sub-microspheres and DOX-eluting patches, 10 mg patches, each containing approximately 160 μg DOX-loaded sub-microspheres, were prepared from a dehydrated film using a biopsy punch (see Figure 1), and placed in a 48-well plate. The patches were hydrated with 50 μL PBS (pH 7.4), and crosslinked for 5 minutes via exposure to visible green light. Subsequently, 500 μL PBS was added to each well, and the entire plate was placed in an incubator shaker at 37°C. At 1, 2, 4, 6, 12, 24, 48 hours, 100 μL of supernatant were collected from each well and immediately replaced with 100 μL of fresh PBS.[29] In addition, 1 mg of sub-microspheres was suspended in 1 mL of PBS, incubated at 37°C; the solution was centrifuged, and the supernatant was analyzed. To quantify cumulative drug released at each time point, the absorbance of collected aliquots was assessed at 485 nm wavelength using a plate reader, and compared to a DOX standard curve.[29, 64] Peak absorbance of DOX in PBS (pH 7.4) was previously confirmed to be 485 nm when assessed using an absorbance spectral sweep from 300–700 nm at 1 mg/mL concentration (Supplemental Figure 1).

2.11. Bioactivity of sub-microspheres and chemotherapeutic patch

The bioactivity of the DOX-eluting patches was assessed using human lung epithelial carcinoma cells (A549, ATCC). Cells were seeded in the lower portion of a 24-well Transwell® plate (0.4 μm pore diameter) at 50,000 cells/well, and allowed to adhere overnight at 37°C in Dulbecco's Modified Eagle Medium: Nutrient Mixture F-12 (DMEM/F-12, Gibco), supplemented with 10% FBS, 100 U/mL penicillin, and 100 μg/mL streptomycin. Prior to starting the assay, 10 mg patches, containing 160 μg of DOX-encapsulating sub-microspheres each, were hydrated and photo-crosslinked on the permeable membrane insert of the Transwell® plate (n=3 per group), and subsequently added to the cell-seeded wells. In addition, 1 mg of sub-microspheres was suspended in 1 mL of PBS, incubated at 37°C; the solution was centrifuged, and the supernatant was analyzed. After 24 hours of culture, viability was assessed as previously described in Section 2.5.

2.12. Statistical analysis

All numerical results are presented as a mean ± standard deviation unless otherwise stated. A one-way ANOVA with Dunnett's method for multiple comparisons was utilized for viability, cytotoxicity, apoptosis, and MTT assays. A one-way ANOVA with Tukey's method for multiple comparisons was used for burst pressure data analysis. A p-value ≤ 0.05 was considered statistically significant for all statistics performed.

3. RESULTS AND DISCUSSION

3.1. Synthesis of AMA and AMA-DA

Methacrylation of alginate was performed to enable covalent photo-crosslinking between adjacent polysaccharide chains in aqueous solutions, forming a

hydrogel.[24, 28–29, 31, 35, 56, 65–71] The aqueous methacrylation chemistry yielded a functionalized biomacromolecule capable of covalent crosslinking, as confirmed by ^{1}H-NMR (Figure 2). Although a 20-molar excess of methacrylic anhydride was utilized for the reaction, the experimental DOM for the AMA utilized in this study was calculated to be 58%. Variances in reaction efficiency are often caused by changes in pH, temperature, alginate solution concentration, and thus 100% modification is not typically observed with this reaction.[56, 72]

Oxidation of AMA using sodium periodate was performed, yielding functional aldehyde groups capable of imine bonding with extracellular matrix proteins. AMA-DA was predicted to have theoretical DOO values of 25% and 50%. Due to variances in reaction efficiency, the calculated, experimental DOO values were calculated to be 19% for AMA-25DA, and 42% for AMA-50DA, respectively. The oxidation efficiencies of both reactions were calculated to be 76% and 84%. The DOM of AMA-DA was again quantified via ^{1}H-NMR to elucidate any reduction in methacrylate side-groups available for photo-crosslinking, as a result of alginate oxidation (Figure 2). The experimental DOMs were found to decline due to the secondary oxidation reaction and were confirmed to be 36% and 38% for AMA-25DA and AMA-50DA respectively.

3.2. Rheology

Viscosity values versus increasing shear rate, for 6% (w/v) alginate-based polymer solutions, are presented in Figure 3A, over a range of increasing shear rates. AMA solutions (blue circles) demonstrated the highest viscosity over all shear rates tested; this was expected, as the AMA materials went through the least amount of chemical processing. Significant decreases in viscosity were observed after oxidation of AMA, as shown by the pure polymer samples, AMA-25DA (red squares) and AMA-50DA (green triangles); viscosity decreased with increasing levels of oxidation, as expected due to the degrading nature of the oxidation reaction. The decrease in viscosity was partially recovered when blended with non-oxidized AMA, as shown by 1:1 blends of AMA:AMA-25DA (orange diamonds) and AMA:AMA-50DA (violet triangles).

3.3. Visible light crosslinking and gelation kinetics

Oscillating a shear force during hydrogel crosslinking reveals the sealants gelation kinetics. Storage modulus, or G', is a measurement of the elastic response of the material, and will increase as crosslinking between adjacent polysaccharide chains and their methacrylate side-groups occurs, resulting in a plateau when crosslinking has reached its terminal maximum. In Figure 3B, G' values are presented and show similar plateauing behavior after 100 seconds for all methacrylated materials. As expected, no increase in storage moduli was observed in non-modified alginate, as no covalent crosslinking or gelation occurred. Non-oxidized AMA exhibited the highest storage moduli after 5 minutes of crosslinking, followed by the AMA-DA blends, and lastly the pure AMA-DA exhibited the lowest moduli.

Pure AMA is inherently non-adhesive, and thus oxidation of the molecule was performed to take advantage of aldehyde-mediated adhesion to proteins commonly found on the tissue

surface. Aldehyde modification of polymers has been shown to improve adhesion to proteins found on or within biological tissues.[35, 43, 54–56, 73–75] Using an oxidation reaction, it is possible to open the uronate residues found on the alginate backbone to form two functional aldehyde groups. There is, however, a balance which must be achieved between the degree of oxidation/aldehyde-modification required to improve sealant adhesion, and the viscosity and mechanical performance of the material. As previously reported, and shown in Figure 3A, the oxidation of alginate and AMA results in significant decreases in solution viscosity as compared to non-modified alginate.[56] This is due to a reduction in molecular weight or chain length of the polysaccharide molecules resulting from the deleterious oxidation reaction.[36, 56] A slight reduction in viscosity was also exhibited by AMA materials, as compared to non-modified alginate, signifying changes in the molecular structure occurred during the initial methacrylation reaction.[56, 76] A reduction in DOM can also be observed when increasing the level of oxidation, as quantified from the ^{1}H-NMR spectra shown in Figure 2. For these reasons, the DOO was kept below 50% for the materials tested in this study. Additionally, the AMA-DA material was blended with non-oxidized AMA to partially recover the viscosity and mechanical performance of the sealant while still maintaining the important presence of aldehyde groups for adhesion. All the patch formulations/blends tested successfully photo-crosslink in under 5 minutes when hydrated and exposed to visible green light (525 nm) as confirmed by the plateauing storage moduli presented in Figure 3B.

3.4. Hydrogel Patch Fabrication

Thin polymer films were successfully formed using an injection molding technique, followed by subsequent lyophilization (Figure 4A,B). These films contain all photo-initiators required for crosslinking to form a hydrogel, when hydrated and exposed to visible green light (Figure 4C). The patches were found to be advantageous from a handling and application perspective, compared with our prior experience utilizing the liquid sealant application. Importantly, the tissue sealant hydrogel patches require no pre-mixing of components, and can be cut to the desired size. The dry patches adhered to moistened surfaces, and hydrated quickly. A tertiary benefit is that the thickness of the patch was consistent and uniform, as it did not flow upon application, which was observed with liquid sealants, applied on non-level surfaces. Due to these factors, clinical applications of these tissue sealant hydrogel patches would be improved as it ameliorates many common issues observed with liquid tissue sealants. Due to the blending of AMA and AMA-DA in the fabrication process (as denoted in Table 1), the DOM and DOO varied between each formulation. The DOM and DOO for each patch formulation was calculated and is listed in Table 1.

3.5. Burst pressure properties

Using a custom-made burst pressure testing device,[62] a wide-range of sealant performance was observed between concentrations and formulations with several achieving burst pressures consistently above the physiological threshold of 12 in H_2O (Figure 5A). A red dotted-line is shown at 12 inH_2O, representing the normal maximum physiological lung pressure, and acts as a threshold which must be achieved for the sealant to be considered for the desired application.[56] Although several 3% and 4.5% (w/v) formulations achieved average burst pressures above this threshold value, the variation (error bars denote standard

deviation) disqualified many of these formulations, as they did not provide any margin of error. AMA, when used alone, was lacking any aldehyde-mediate adhesion, and thus was prone to delamination or adhesive failure. Sealant patch formulations that were prone to delamination, yielded the highest levels of variation between samples. Groups which consistently yielded burst pressures above this threshold, with acceptable levels of variation, were the 6% (w/v) formulations, of which the AMA:AMA-25DA, 1:1 blend, performed significantly better than the other 6% (w/v) formulations, with an average burst pressure above 200 in-H_2O. Sealant patches containing AMA and AMA-DA at 1:1 or 1:2 ratio fail almost exclusively via material failure, or rupture (Table 1), which is believed to be due to improved adhesion to the collagen substrate as well as weakened mechanical performance (Figure 3B).

The mechanism of sealant failure was assessed using high-speed videography. Material failure occurred when a rupture was formed through the sealant material, while the sealant maintained adhesion to the substrate, as indicated in Figure 5B, by a small perforation. Adhesive failure, or delamination, occurred when the sealant peeled from the substrate, either partially or completely (as shown in Figure 5C). The predominant mode of failure for each patch formulation is listed in Table 1. Sealants blended with AMA-DA were more prone to material failure (rupture), verifying good adhesion, while pure AMA-based sealants failed exclusively through adhesive failure (delamination) due to lack of crosslinking to the substrate. Blends of AMA and AMA-DA at a 1:2 ratio failed predominantly via material failure, though reverted to adhesive failure when blended at an inverse ratio of 2:1.

3.6. Degradation of alginate-based sealant patches

Swell ratios also decreased significantly during the 14-day period (Figure 6A), from 2667% to 1902%, which relates to the decrease in water-retaining polysaccharide content. Over a 14-day period, 6% (w/v) AMA:AMA-25DA blended at a 1:1 ratio, lost greater than 50% of their initial dry mass (Figure 6B). Visual changes in appearance can also be observed, from Day 1 (Figure 6C), with pitting and surface erosion observed on the hydrogel patch surfaces (Figure 6D). As the typical timeframe for healing of non-chronic pneumothorax ranges from 1–2 weeks in most cases, with treatment, the degradation of this material aligns well with the expected tissue regeneration occurring during this period.[4] As the underlying tissue regenerates, the need for continued mechanical support from the sealant patch is expected to diminish. Future studies will investigate how this degradation process effects sealant patch mechanics and adhesion, so that the rate of degradation can be tuned to match the rate of tissue regeneration.

3.7. Material cytotoxicity, healthy cell viability, and apoptosis analysis

Mesothelial cells are one of the predominant cell types found in pleural tissues, and thus were utilized to assess material cytotoxicity. After 24 hours of exposure to the hydrogel patch materials (not containing DOX), no statistically significant decreases in MeT-5A human mesothelial cell viability were observed (Figure 7A), though significant increases in cell viability were witnessed by the cells exposed to AMA and AMA-50DA. These increases in viability are attributed to the release of low molecular weight polysaccharide molecules from the material into the culture medium during degradation, which may provide an

additional source of nutrients for the cells and effect cell metabolism and proliferation.[77] Indeed, though no significant increases in cytotoxicity were observed in the cells exposed to sealant materials, significant decreases in cytotoxicity are shown in both AMA and AMA-50DA groups (Figure 7B) which correlated with cell viability results. Cell metabolism as indicated by mitochondrial activity is often used as an indicator of cytotoxicity and proliferation using MTT-based assays.[29, 58, 78–80] MTT is metabolized by the cell mitochondria resulting in the formation of formazan crystals which can subsequently be dissolved and quantified via absorbance detection on a plate reader. Increased formazan concentrations result in heightened absorbance, signifying higher mitochondrial activity, and decreased cytotoxicity. No significant differences in MeT-5A human mesothelial cell apoptosis or mitochondrial activity were found for any of the novel alginate-based hydrogel sealant materials (Figure 7C,D).

3.8. DOX-loaded sealant patches and mechanisms of drug release

DOX-loaded AMA sub-microspheres were successfully synthesized using a water-in-oil emulsion technique. Size distribution was assessed by DLS. Sub-microspheres were found to be under 200 nm diameter in general, with the peak size being 150 nm in diameter (Figure 8A). Encapsulation efficiency [EE, EE = (actual DOX encapsulated)/(theoretical DOX encapsulated)] was calculated to be 28%, as described in our prior study. Drug release profiles for DOX-loaded chemotherapeutic sealant patches, and DOX-loaded AMA sub-microspheres, were assessed over 48 hours (Figure 8B); drug release quantities were reported in (mg DOX)/(mg sub-microspheres), and as a percent of the encapsulated DOX (right axis). During the initial 12 hours, the drug release expressed by the DOX-loaded AMA sub-microspheres occurred more rapidly, while the chemotherapeutic sealant patches exhibited delayed DOX release. After a total of 48 hours, no significant differences were calculated in the total amount of DOX released by any test group.

3.9 Anti-cancer activity of DOX-loaded sealant patches

The bioactivity of DOX-eluting alginate-based sealant patches, as compared to DOX-loaded AMA sub-microspheres, and non-loaded patches, was assessed using A549 cells, after 24-hour exposure to the test materials, and reported as viability in Figure 8B. No decrease in viability was observed after 24 hours of cell exposure to non-DOX-loaded patch materials, whereas a significant decrease in cell viability was demonstrated by both DOX-eluting patch formulations tested. No significant reduction in A549 viability was observed under treatment with DOX sub-microspheres alone (Figure 8B).

Alginate-based materials are commonly utilized, and increasingly so, in biological and medical applications and are widely accepted as highly biocompatible. Indeed, mesothelial cells demonstrated no deleterious effects when cultured in the presence of alginate sealant patch materials over 24 hours, as confirmed by viability, cytotoxicity, apoptosis and mitochondrial activity assays (Figure 8). Inversely, when DOX-loaded AMA sub-microspheres were incorporated into the adhesive patch, and cultured with A549 human lung cancer cells, cell viability significantly decreased, revealing a potential application as a drug-eluting tissue sealant. As the sub-microspheres are made from the same AMA material as the sealant, the sub-microspheres are seamlessly photo-crosslinked within the hydrogel

sealant. Drug release assays revealed a delayed DOX release from the drug-eluting sealant patches as compared to sub-microspheres alone (Figure 8C). This is hypothesized to be the results of the drug, which has a relatively low solubility in aqueous solutions, diffusing not only through the sub-microspheres but subsequently through the surrounding sealant hydrogel, before ultimately diffusing into the surrounding aqueous environment. This bi-phasic drug diffusion process, initially through the particle and subsequently through the patch, delays drug release from the drug-eluting patch, as compared to the sub-microspheres alone. Interestingly, although the DOX-loaded sub-microspheres released drug more rapidly than DOX-eluting sealant patches, they appear less effective in reducing cancer cell viability over a 24-hour period (Figure 8B). Due to the small size of these sub-microspheres, approximately 150 nm in diameter, and prior research performed using similar particles, it is hypothesized that many of the particles within the culture are rapidly internalized by A549 cells.[29] In prior studies, efficacy of DOX-encapsulating particles in clearing cancer cell populations improved over a 5-day period, and it was hypothesized that once internalized, the particle and drug may be temporarily trapped within an endosome, and not be immediately available to act on the cell nuclei and DNA.[29, 63, 81] The pH within an endosome can also vary significantly from that of the cell culture media, also influencing drug release. Decreasing pH can induce protonation of the carboxylate side groups on the alginate backbone, causing hydrogen bonding to occur and an increase in viscosity, ultimately slowing diffusion processes further in internalized sub-microspheres.[27] Based upon these results, assessing bioactivity of DOX-eluting tissue sealant patches and sub-microspheres over an extended period of time will be a focus of future studies, to establish critical time-frames for drug release and tune release kinetics accordingly.

4. CONCLUSIONS

Alginate-based hydrogel sealant patches were successfully designed and fabricated, using visible green light induced crosslinking. AMA materials required moderate aldehyde modification to improve adhesive properties of the hydrogel material. Blending of non-oxidized material with oxidized (i.e., aldehyde modified) alginates yielded sealant patches with improved burst pressure performance, and decreased delamination as compared to pure AMA. Anti-cancer drug-eluting sealant patches also demonstrated efficacy when loaded with DOX-encapsulating sub-microspheres, and cultured in the presence of A549 human lung cancer cells, suggesting diversified medical applications.

Supplementary Material

Refer to Web version on PubMed Central for supplementary material.

Acknowledgments

This work was funded in part by NIH Grants T32 HL076122 (SL Fenn training fellowship), R01 EB020964-01 (Oldinski), The University of Vermont SPARK^{VT} Program, as well as the University of Vermont College of Engineering and Mathematical Sciences.

References

1. Huang Y, Huang H, Li Q, Browning RF, Parrish S, Turner JF Jr, Zarogoulidis K, Kougioumtzi I, Dryllis G, Kioumis I, Pitsiou G, Machairiotis N, Katsikogiannis N, Courcoutsakis N, Madesis A, Diplaris K, Karaiskos T, Zarogoulidis P. Approach of the Treatment for Pneumothorax. J Thorac Dis. 2014; 6(Suppl 4):S416–420. [PubMed: 25337397]
2. Trump M, Gohar A. Diagnosis and Treatment of Pneumothorax. Hosp Pract. 2013; 41(3):28–39.
3. Pawloski DR, Broaddus KD. Pneumothorax: A Review. J Am Anim Hosp Assoc. 2010; 46(6):385–397. [PubMed: 21041331]
4. Zarogoulidis P, Kioumis I, Pitsiou G, Porpodis K, Lampaki S, Papaiwannou A, Katsikogiannis N, Zaric B, Branislav P, Secen N, Dryllis G, Machairiotis N, Rapti A, Zarogoulidis K. Pneumothorax: From Definition to Diagnosis and Treatment. J Thorac Dis. 2014; 6(Suppl 4):S372–376. [PubMed: 25337391]
5. McPherson JJ, Feigin DS, Bellamy RF. Prevalence of Tension Pneumothorax in Fatally Wounded Combat Casualties. J Trauma. 2006; 60(3):573–578. [PubMed: 16531856]
6. Harrison M. Traumatic Pneumothorax: A Review of Current Practices. Br J Hosp Med. 2014; 75(3): 132–135.
7. Van Schil PE. Treatment of Pneumothorax: Minimally or Maximally Invasive? Eur J Cardiothorac Surg. 2016; 49(3):868–869. [PubMed: 26164262]
8. Nkere UU, Griffin SC, Fountain SW. Pleural Abrasion: A New Method of Pleurodesis. Thorax. 1991; 46(8):596–598. [PubMed: 1926032]
9. Zimmer PW, Hill M, Casey K, Harvey E, Low DE. Prospective Randomized Trial of Talc Slurry Vs Bleomycin in Pleurodesis for Symptomatic Malignant Pleural Effusions. Chest. 1997; 112(2):430–434. [PubMed: 9266880]
10. Kennedy L, Sahn SA. Talc Pleurodesis for the Treatment of Pneumothorax and Pleural Effusion. Chest. 1994; 106(4):1215–1222. [PubMed: 7924497]
11. Ranger WR, Halpin D, Sawhney AS, Lyman M, Locicero J. Pneumostasis of Experimental Air Leaks with a New Photopolymerized Synthetic Tissue Sealant. Am Surg. 1997; 63(9):788–795. [PubMed: 9290523]
12. Wain JC, Kaiser LR, Johnstone DW, Yang SC, Wright CD, Friedberg JS, Feins RH, Heitmiller RF, Mathisen DJ, Selwyn MR. Trial of a Novel Synthetic Sealant in Preventing Air Leaks after Lung Resection. The Annals of Thoracic Surgery. 2001; 71(5):1623–1629. [PubMed: 11383811]
13. Klijian A. A Novel Approach to Control Air Leaks in Complex Lung Surgery: A Retrospective Review. J Cardiothorac Surg. 2012; 7:49. [PubMed: 22657101]
14. Fuller C. Reduction of Intraoperative Air Leaks with Progel in Pulmonary Resection: A Comprehensive Review. J Cardiothorac Surg. 2013; 8:90. [PubMed: 23590942]
15. Ibrahim M, Pindozzi F, Menna C, Rendina EA. Intraoperative Bronchial Stump Air Leak Control by Progel(R) Application after Pulmonary Lobectomy. Interact Cardiovasc Thorac Surg. 2016; 22(2):222–224. [PubMed: 26541960]
16. Haj-Yahia S, Mittal T, Birks E, Carby M, Petrou M, Pepper J, Dreyfus G, Amrani M. Lung Fibrosis as a Potential Complication of the Hemostatic Tissue Sealant, Biologic Glue (Bioglue). J Thorac Cardiovasc Surg. 2007; 133(5):1387–1388. [PubMed: 17467473]
17. Araki M, Tao H, Nakajima N, Sugai H, Sato T, Hyon SH, Nagayasu T, Nakamura T. Development of New Biodegradable Hydrogel Glue for Preventing Alveolar Air Leakage. J Thorac Cardiovasc Surg. 2007; 134(5):1241–1248. [PubMed: 17976456]
18. Browdie DA, Cox D. Tests of Experimental Tissue Adhesive Sealants: Analysis of Strength Effects in Relation to Tissue Adhesive Sealant Standards. Tex Heart Inst J. 2007; 34(3):313–317. [PubMed: 17948082]
19. Saxena AK. Synthetic Biodegradable Hydrogel (Pleuraseal) Sealant for Sealing of Lung Tissue after Thoracoscopic Resection. J Thorac Cardiovasc Surg. 2010; 139(2):496–497. [PubMed: 19660330]
20. Elvin CM, Vuocolo T, Brownlee AG, Sando L, Huson MG, Liyou NE, Stockwell PR, Lyons RE, Kim M, Edwards GA, Johnson G, McFarland GA, Ramshaw JA, Werkmeister JA. A Highly

Elastic Tissue Sealant Based on Photopolymerised Gelatin. Biomaterials. 2010; 31(32):8323–8331. [PubMed: 20674967]

21. Spotnitz WD, Prabhu R. Fibrin Sealant Tissue Adhesive–Review and Update. J Long Term Eff Med Implants. 2005; 15(3):245–270. [PubMed: 16022636]
22. Committee AT, Bhat YM, Banerjee S, Barth BA, Chauhan SS, Gottlieb KT, Konda V, Maple JT, Murad FM, Pfau PR, Pleskow DK, Siddiqui UD, Tokar JL, Wang A, Rodriguez SA. Tissue Adhesives: Cyanoacrylate Glue and Fibrin Sealant. Gastrointest Endosc. 2013; 78(2):209–215. [PubMed: 23867370]
23. Braunwald NS, Gay W, Tatooles CJ. Evaluation of Crosslinked Gelatin as a Tissue Adhesive and Hemostatic Agent - an Experimental Study. Surgery. 1966; 59(6):1024–+. [PubMed: 5937947]
24. Wagner DE, Fenn SL, Bonenfant NR, Marks ER, Borg Z, Saunders P, Oldinski RA, Weiss DJ. Design and Synthesis of an Artificial Pulmonary Pleura for High Throughput Studies in Acellular Human Lungs. Cell Mol Bioeng. 2014; 7(2):184–195. [PubMed: 25750684]
25. Lee KY, Mooney DJ. Hydrogels for Tissue Engineering. Chem Rev. 2001; 101(7):1869–1880. [PubMed: 11710233]
26. Zhao X, Huebsch N, Mooney DJ, Suo Z. Stress-Relaxation Behavior in Gels with Ionic and Covalent Crosslinks. J Appl Phys. 2010; 107(6):63509. [PubMed: 21464912]
27. Lee KY, Mooney DJ. Alginate: Properties and Biomedical Applications. Prog Polym Sci. 2012; 37(1):106–126. [PubMed: 22125349]
28. Moller L, Krause A, Dahlmann J, Gruh I, Kirschning A, Drager G. Preparation and Evaluation of Hydrogel-Composites from Methacrylated Hyaluronic Acid, Alginate, and Gelatin for Tissue Engineering. Int J Artif Organs. 2011; 34(2):93–102. [PubMed: 21374568]
29. Fenn SL, Miao T, Scherrer RM, Oldinski RA. Dual-Cross-Linked Methacrylated Alginate Sub-Microspheres for Intracellular Chemotherapeutic Delivery. ACS Appl Mater Interfaces. 2016; 8(28):17775–17783. [PubMed: 27378419]
30. Chou AI, Akintoye SO, Nicoll SB. Photo-Crosslinked Alginate Hydrogels Support Enhanced Matrix Accumulation by Nucleus Pulposus Cells in Vivo. Osteoarthr Cartil. 2009; 17(10):1377–1384. [PubMed: 19427928]
31. Jeon O, Bouhadir KH, Mansour JM, Alsberg E. Photocrosslinked Alginate Hydrogels with Tunable Biodegradation Rates and Mechanical Properties. Biomaterials. 2009; 30(14):2724–2734. [PubMed: 19201462]
32. Jeon O, Alsberg E. Photofunctionalization of Alginate Hydrogels to Promote Adhesion and Proliferation of Human Mesenchymal Stem Cells. Tissue engineering Part A. 2013; 19(11–12): 1424–1432. [PubMed: 23327676]
33. Gao C, Liu M, Chen S, Jin S, Chen J. Preparation of Oxidized Sodium Alginate-Graft-Poly((2-Dimethylamino) Ethyl Methacrylate) Gel Beads and in Vitro Controlled Release Behavior of Bsa. Int J Pharm (Amsterdam, Neth). 2009; 371(1–2):16–24.
34. Balakrishnan B, Lesieur S, Labarre D, Jayakrishnan A. Periodate Oxidation of Sodium Alginate in Water and in Ethanol-Water Mixture: A Comparative Study. Carbohydr Res. 2005; 340(7):1425–1429. [PubMed: 15854617]
35. Jeon O, Samorezov JE, Alsberg E. Single and Dual Crosslinked Oxidized Methacrylated Alginate/Peg Hydrogels for Bioadhesive Applications. Acta Biomater. 2014; 10(1):47–55. [PubMed: 24035886]
36. Jeon O, Alt DS, Ahmed SM, Alsberg E. The Effect of Oxidation on the Degradation of Photocrosslinkable Alginate Hydrogels. Biomaterials. 2012; 33(13):3503–3514. [PubMed: 22336294]
37. Kim WS, Mooney DJ, Arany PR, Lee K, Huebsch N, Kim J. Adipose Tissue Engineering Using Injectable, Oxidized Alginate Hydrogels. Tissue engineering. Part A. 2012; 18(7–8):737–743. [PubMed: 22011105]
38. Rayatpisheh S, Poon YF, Cao Y, Feng J, Chan V, Chan-Park MB. Aligned 3d Human Aortic Smooth Muscle Tissue Via Layer by Layer Technique inside Microchannels with Novel Combination of Collagen and Oxidized Alginate Hydrogel. J Biomed Mater Res Part A. 2011; 98(2):235–244.

39. Linh NT, Paul K, Kim B, Lee BT. Augmenting in Vitro Osteogenesis of a Glycine-Arginine-Glycine-Aspartic-Conjugated Oxidized Alginate-Gelatin-Biphasic Calcium Phosphate Hydrogel Composite and in Vivo Bone Biogenesis through Stem Cell Delivery. J Biomater Appl. 2016; 31(5):661–673. [PubMed: 27604088]
40. Park H, Lee KY. Cartilage Regeneration Using Biodegradable Oxidized Alginate/Hyaluronate Hydrogels. J Biomed Mater Res Part A. 2014; 102(12):4519–4525.
41. Baniasadi H, Mashayekhan S, Fadaoddini S, Haghirsharifzamini Y. Design, Fabrication and Characterization of Oxidized Alginate-Gelatin Hydrogels for Muscle Tissue Engineering Applications. J Biomater Appl. 2016; 31(1):152–161. [PubMed: 26916948]
42. Liao H, Zhang H, Chen W. Differential Physical, Rheological, and Biological Properties of Rapid in Situ Gelable Hydrogels Composed of Oxidized Alginate and Gelatin Derived from Marine or Porcine Sources. J Mater Sci: Mater Med. 2009; 20(6):1263–1271. [PubMed: 19184370]
43. Balakrishnan B, Mohanty M, Umashankar PR, Jayakrishnan A. Evaluation of an in Situ Forming Hydrogel Wound Dressing Based on Oxidized Alginate and Gelatin. Biomaterials. 2005; 26(32): 6335–6342. [PubMed: 15919113]
44. Balakrishnan B, Mohanty M, Fernandez AC, Mohanan PV, Jayakrishnan A. Evaluation of the Effect of Incorporation of Dibutyryl Cyclic Adenosine Monophosphate in an in Situ-Forming Hydrogel Wound Dressing Based on Oxidized Alginate and Gelatin. Biomaterials. 2006; 27(8): 1355–1361. [PubMed: 16146648]
45. Nguyen TP, Lee BT. Fabrication of Oxidized Alginate-Gelatin-Bcp Hydrogels and Evaluation of the Microstructure, Material Properties and Biocompatibility for Bone Tissue Regeneration. J Biomater Appl. 2012; 27(3):311–321. [PubMed: 21680610]
46. Zeng Q, Chen W. The Functional Behavior of a Macrophage/Fibroblast Co-Culture Model Derived from Normal and Diabetic Mice with a Marine Gelatin-Oxidized Alginate Hydrogel. Biomaterials. 2010; 31(22):5772–5781. [PubMed: 20452666]
47. Sarker A, Amirian J, Min YK, Lee BT. Hap Granules Encapsulated Oxidized Alginate-Gelatin-Biphasic Calcium Phosphate Hydrogel for Bone Regeneration. Int J Biol Macromol. 2015; 81:898–911. [PubMed: 26394381]
48. Zhang H, Liao H, Chen W. In Situ Gelable Glycation-Resistant Hydrogels Composed of Gelatin and Oxidized Alginate. J Biomater Sci Polym Ed. 2010; 21(3):329–342. [PubMed: 20178689]
49. Li X, Chen S, Zhang B, Li M, Diao K, Zhang Z, Li J, Xu Y, Wang X, Chen H. In Situ Injectable Nano-Composite Hydrogel Composed of Curcumin, N,O-Carboxymethyl Chitosan and Oxidized Alginate for Wound Healing Application. Int J Pharm. 2012; 437(1–2):110–119. [PubMed: 22903048]
50. Wright B, De Bank PA, Luetchford KA, Acosta FR, Connon CJ. Oxidized Alginate Hydrogels as Niche Environments for Corneal Epithelial Cells. J Biomed Mater Res Part A. 2014; 102(10): 3393–3400.
51. Sakai S, Yamaguchi S, Takei T, Kawakami K. Oxidized Alginate-Cross-Linked Alginate/Gelatin Hydrogel Fibers for Fabricating Tubular Constructs with Layered Smooth Muscle Cells and Endothelial Cells in Collagen Gels. Biomacromolecules. 2008; 9(7):2036–2041. [PubMed: 18537290]
52. Balakrishnan B, Joshi N, Jayakrishnan A, Banerjee R. Self-Crosslinked Oxidized Alginate/Gelatin Hydrogel as Injectable, Adhesive Biomimetic Scaffolds for Cartilage Regeneration. Acta Biomater. 2014; 10(8):3650–3663. [PubMed: 24811827]
53. Wang Y, Peng W, Liu X, Zhu M, Sun T, Peng Q, Zeng Y, Feng B, Zhi W, Weng J, Wang J. Study of Bilineage Differentiation of Human-Bone-Marrow-Derived Mesenchymal Stem Cells in Oxidized Sodium Alginate/N-Succinyl Chitosan Hydrogels and Synergistic Effects of Rgd Modification and Low-Intensity Pulsed Ultrasound. Acta Biomater. 2014; 10(6):2518–2528. [PubMed: 24394634]
54. Bouhadir KH, Lee KY, Alsberg E, Damm KL, Anderson KW, Mooney DJ. Degradation of Partially Oxidized Alginate and Its Potential Application for Tissue Engineering. Biotechnol Prog. 2001; 17(5):945–950. [PubMed: 11587588]
55. Manju S, Muraleedharan CV, Rajeev A, Jayakrishnan A, Joseph R. Evaluation of Alginate Dialdehyde Cross-Linked Gelatin Hydrogel as a Biodegradable Sealant for Polyester Vascular Graft. J Biomed Mater Res Part B. 2011; 98(1):139–149.

56. Charron PN, Fenn SL, Poniz A, Oldinski RA. Mechanical Properties and Failure Analysis of Visible Light Crosslinked Alginate-Based Tissue Sealants. J Mech Behav Biomed Mater. 2016; 59:314–321. [PubMed: 26897093]
57. Gomez CG, Rinaudo M, Villar MA. Oxidation of Sodium Alginate and Characterization of the Oxidized Derivatives. Carbohyd Polym. 2007; 67(3):296–304.
58. Fenn SL, Oldinski RA. Visible Light Crosslinking of Methacrylated Hyaluronan Hydrogels for Injectable Tissue Repair. J Biomed Mater Res Part B. 2016; 104(6):1229–1236.
59. Nettles DL, Vail TP, Morgan MT, Grinstaff MW, Setton LA. Photocrosslinkable Hyaluronan as a Scaffold for Articular Cartilage Repair. Ann Biomed Eng. 2004; 32(3):391–397. [PubMed: 15095813]
60. Smeds KA, Pfister-Serres A, Miki D, Dastgheib K, Inoue M, Hatchell DL, Grinstaff MW. Photocrosslinkable Polysaccharides for in Situ Hydrogel Formation. J Biomed Mater Res. 2001; 54(1):115–121. [PubMed: 11077410]
61. Park YD, Tirelli N, Hubbell JA. Photopolymerized Hyaluronic Acid-Based Hydrogels and Interpenetrating Networks. Biomaterials. 2003; 24(6):893–900. [PubMed: 12504509]
62. ASTM-F2392-04, Standard Test Method for Burst Strength of Surgical Sealants. Annu Book ASTM Stand. 2015
63. Miao T, Rao KS, Spees JL, Oldinski RA. Osteogenic Differentiation of Human Mesenchymal Stem Cells through Alginate-Graft-Poly(Ethylene Glycol) Microsphere-Mediated Intracellular Growth Factor Delivery. J Controlled Release. 2014; 192:57–66.
64. Saraswathy M, Knight GT, Pilla S, Ashton RS, Gong S. Multifunctional Drug Nanocarriers Formed by Crgd-Conjugated Betacd-Pamam-Peg for Targeted Cancer Therapy. Colloids Surf B. 2015; 126:590–597.
65. Jeon O, Wolfson DW, Alsberg E. In-Situ Formation of Growth-Factor-Loaded Coacervate Microparticle-Embedded Hydrogels for Directing Encapsulated Stem Cell Fate. Adv Mater. 2015; 27(13):2216–2223. [PubMed: 25708428]
66. Kang LH, Armstrong PA, Lee LJ, Duan B, Kang KH, Butcher JT. Optimizing Photo-Encapsulation Viability of Heart Valve Cell Types in 3d Printable Composite Hydrogels. Ann Biomed Eng. 2017; 45(2):360–377. [PubMed: 27106636]
67. Mignon A, Devisscher D, Graulus GJ, Stubbe B, Martins J, Dubruel P, De Belie N, Van Vlierberghe S. Combinatory Approach of Methacrylated Alginate and Acid Monomers for Concrete Applications. Carbohyd Polym. 2017; 155:448–455.
68. Mu C, Sakai S, Ijima H, Kawakami K. Preparation of Cell-Enclosing Microcapsules through Photopolymerization of Methacrylated Alginate Solution Triggered by Irradiation with Visible Light. J Biosci Bioeng. 2010; 109(6):618–621. [PubMed: 20471603]
69. Samorezov JE, Morlock CM, Alsberg E. Dual Ionic and Photo-Crosslinked Alginate Hydrogels for Micropatterned Spatial Control of Material Properties and Cell Behavior. Bioconjugate Chem. 2015; 26(7):1339–1347.
70. Wang S, Jeon O, Shankles PG, Liu Y, Alsberg E, Retterer ST, Lee BP, Choi CK. In-Situ Photopolymerization of Monodisperse and Discoid Oxidized Methacrylated Alginate Microgels in a Microfluidic Channel. Biomicrofluidics. 2016; 10(1):011101. [PubMed: 26865901]
71. Zhao J, Zhao X, Guo B, Ma PX. Multifunctional Interpenetrating Polymer Network Hydrogels Based on Methacrylated Alginate for the Delivery of Small Molecule Drugs and Sustained Release of Protein. Biomacromolecules. 2014; 15(9):3246–3252. [PubMed: 25102223]
72. Smeds KA, Pfister-Serres A, Miki D, Dastgheib K, Inoue M, Hatchell DL, Grinstaff MW. Photocrosslinkable Polysaccharides for in Situ Hydrogel Formation. J Biomed Mater Res. 2001; 54(1):115–121. [PubMed: 11077410]
73. Duan B, Hockaday LA, Kapetanovic E, Kang KH, Butcher JT. Stiffness and Adhesivity Control Aortic Valve Interstitial Cell Behavior within Hyaluronic Acid Based Hydrogels. Acta Biomater. 2013; 9(8):7640–7650. [PubMed: 23648571]
74. Petratos PB, Ito K, Felsen D, Poppas D. Cross-Linked Matrix Tissue Sealant Protects against Mortality and Hemorrhage in an Acute Renal Injury Model in Heparinized Rats. J Urol. 2002; 167(5):2222–2224. [PubMed: 11956482]

75. Shinya N, Oka S, Miyabashira S, Kaetsu H, Uchida T, Sueyoshi M, Takase K, Akuzawa M, Miyamoto A, Shigaki T. Improvement of the Tissue-Adhesive and Sealing Effect of Fibrin Sealant Using Polyglycolic Acid Felt. J Invest Surg. 2009; 22(5):383–389. [PubMed: 19842894]

76. Fenn SL, Oldinski RA. Visible Light Crosslinking of Methacrylated Hyaluronan Hydrogels for Injectable Tissue Repair. J Biomed Mater Res B Appl Biomater. 2015

77. Bohari SP, Hukins DW, Grover LM. Effect of Calcium Alginate Concentration on Viability and Proliferation of Encapsulated Fibroblasts. Biomed Mater Eng. 2011; 21(3):159–170. [PubMed: 22072080]

78. Yan X, Gemeinhart RA. Cisplatin Delivery from Poly(Acrylic Acid-Co-Methyl Methacrylate) Microparticles. J Controlled Release. 2005; 106(1–2):198–208.

79. Miao T, Miller EJ, McKenzie C, Oldinski RA. Physically Crosslinked Polyvinyl Alcohol and Gelatin Interpenetrating Polymer Network Theta-Gels for Cartilage Regeneration. J Mater Chem B. 2015; 3(48):9242–9249.

80. Miao T, Fenn SL, Charron PN, Oldinski RA. Self-Healing and Thermoresponsive Dual-Cross-Linked Alginate Hydrogels Based on Supramolecular Inclusion Complexes. Biomacromolecules. 2015; 16(12):3740–3750. [PubMed: 26509214]

81. Gratton SE, Ropp PA, Pohlhaus PD, Luft JC, Madden VJ, Napier ME, DeSimone JM. The Effect of Particle Design on Cellular Internalization Pathways. Proc Natl Acad Sci U S A. 2008; 105(33): 11613–11618. [PubMed: 18697944]

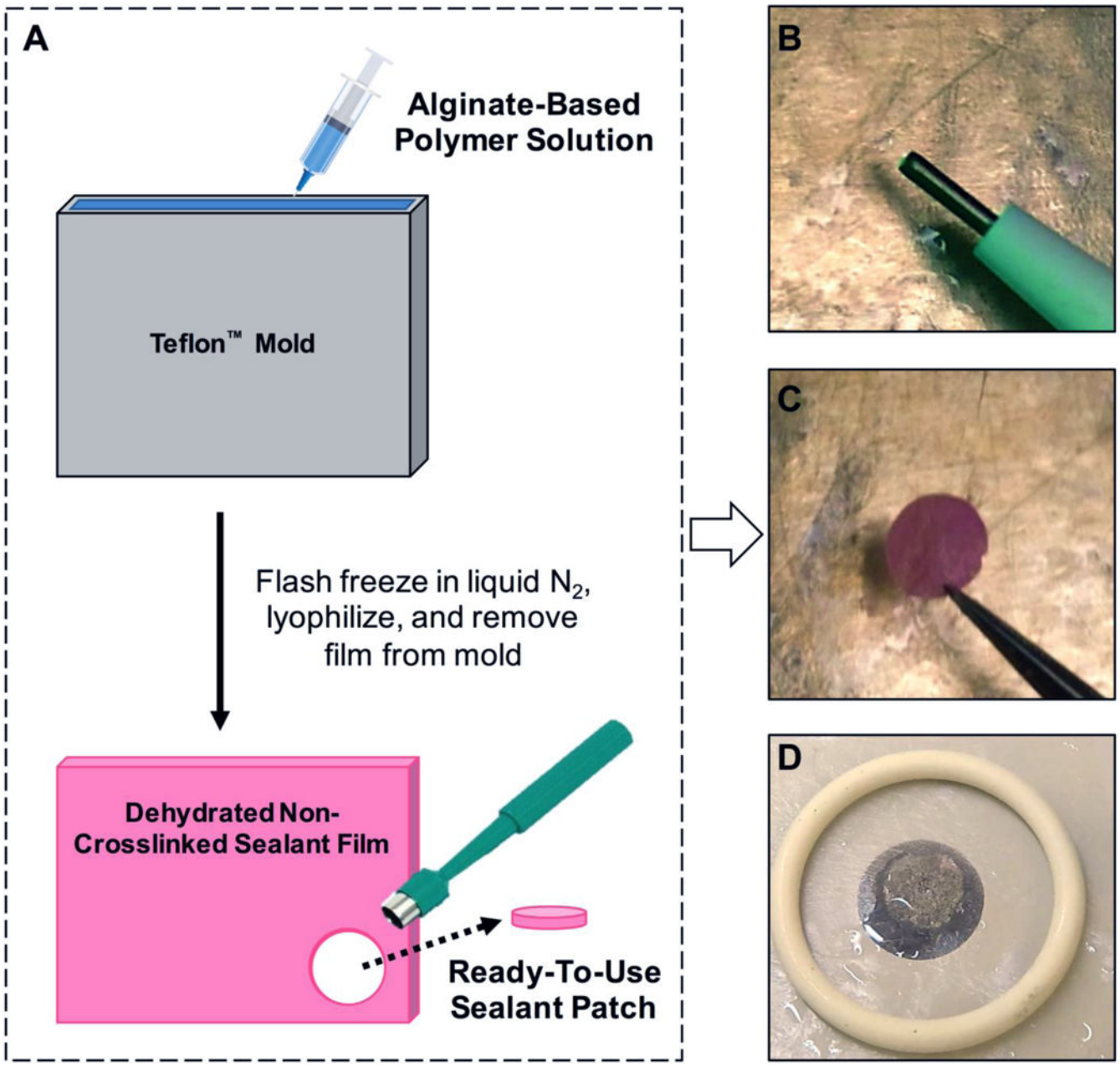

Figure 1.

(A) Fabrication and manufacturing of tissue sealant patches using an injection molding technique. In combination with lyophilization, dehydrated films of alginate-based sealant materials were formed. Circular, thin, non-crosslinked sealant patches were prepared using a biopsy punch. (B) A 1.5 mm diameter defect was created in the collagen membrane using a biopsy punch. (C) Over these defects, 8 mm diameter sealant patches were applied to the membrane and photo-crosslinked. (D) The sealed membrane was then placed on the burst-pressure testing apparatus.

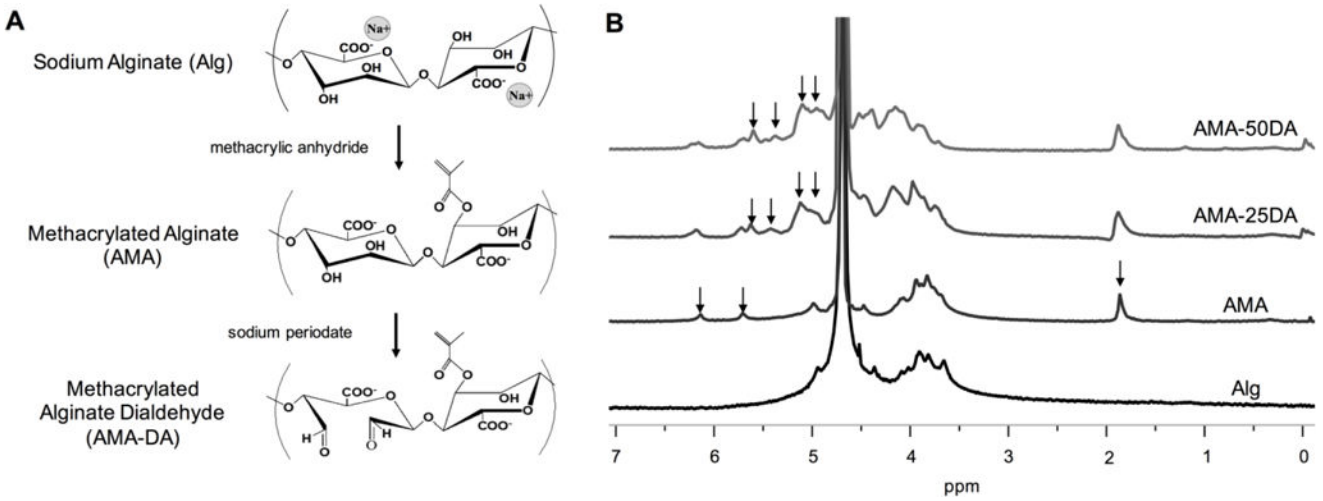

Figure 2.

(A) Molecular repeat units for sodium alginate (Alg), methacrylated alginate (AMA), and methacrylated and oxidized alginate (AMA-DA) are presented. (B) The ^{1}H-NMR spectra of 25% and 50% oxidized AMA-DA, AMA and unmodified alginate are shown as labelled. Peaks of interest identified with arrows. The peaks at 5.78 and 6.24 ppm indicate that the hydrogens on the methylene of the methacrylate groups were present on the alginate backbone after modification. The DOM for AMA was calculated to be 58%. The peaks at 5.17, 5.48, and 5.68 ppm are indicative of oxidation and the formation of aldehyde groups. The experimental DOO for the AMA-25DA and AMA-50DA groups were calculated to be 19% and 42%, respectively The DOM decreased after oxidation, down to 38% and 36%, respectively.

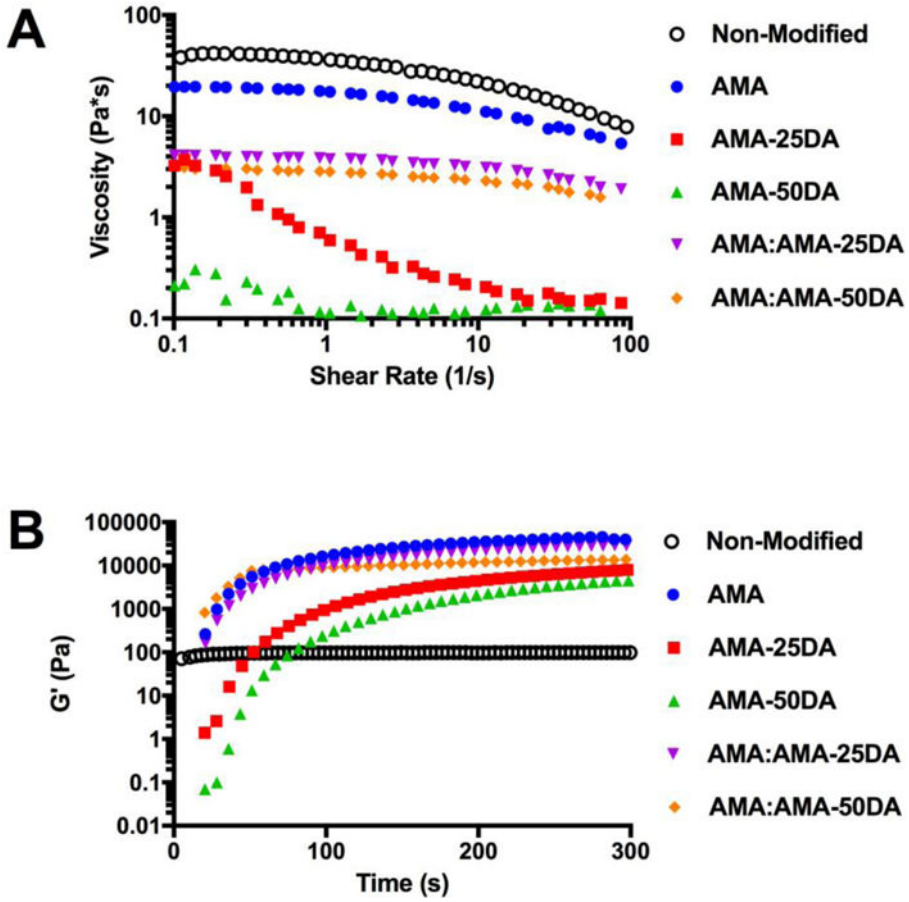

Figure 3.

(A) Viscosity (Pa*s) of 6% (w/v) alginate-based solutions was assessed over shear rates of 1–100 (1/s) at 37°C. Viscosity decreased for the oxidized alginate (i.e., AMA-DA) solutions, but was partially recovered after blending with AMA (1:1 weight ratio). (B) Gelation kinetics were assessed by oscillatory time sweeps at 10% radial strain and 1 Hz, while hydrogel pre-cursor solutions were exposed to visible green light (525 nm) for a total of 5 minutes. Storage moduli (G′) are graphed for pure polymer solutions and polymer blends.

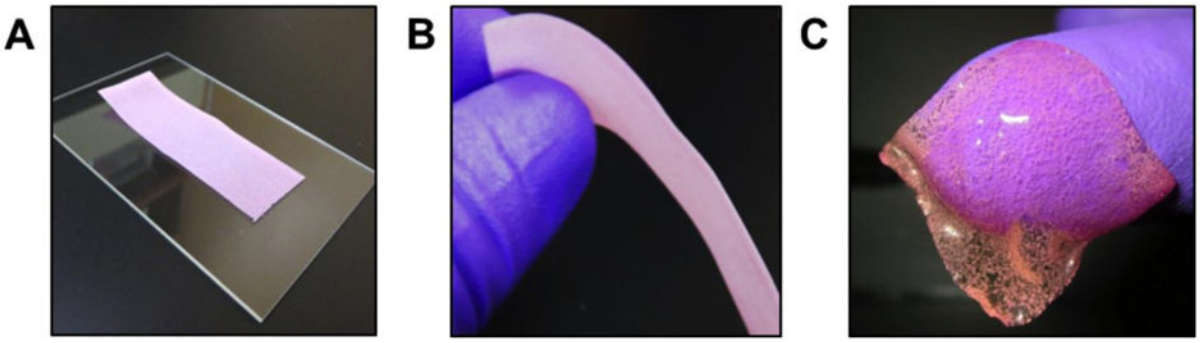

Figure 4.

(A,B) Dry films of non-crosslinked alginate-based sealant material after injection molding and lyophilization, incorporating all required initiators for visible green light photo-crosslinking. (C) Hydrated, and crosslinked, alginate-based hydrogel sealant.

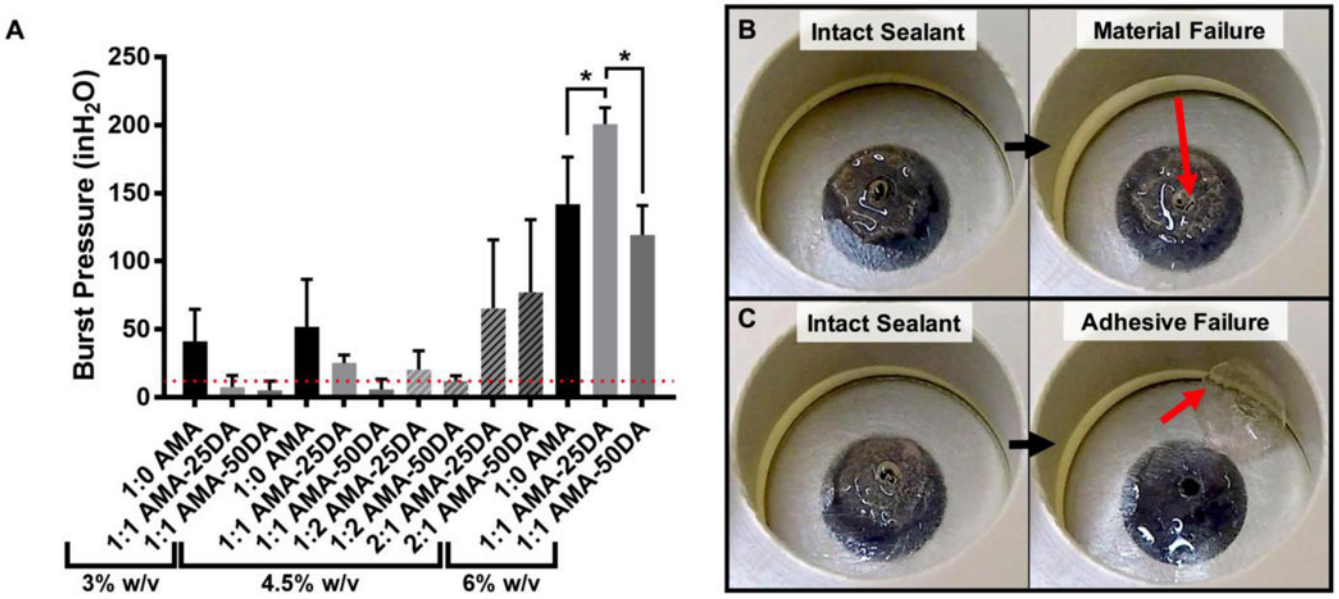

Figure 5.

(A) Burst pressure values for alginate-based tissue sealants, at failure, are shown for all tested formulations as inH_2O. Physiological lung pressures typically remain below 12 inH_2O, which is denoted with a red dotted-line. Statistical significance ($p \leq 0.05$) is shown between specific groups using an asterisk. (B) Image of material failure, which occurred when a rupture was formed through the sealant material, while the patch remained adhered to the underlying substrate. (C) Image of adhesive failure which occurred when the patch delaminated, either partially or completely, from the substrate beneath.

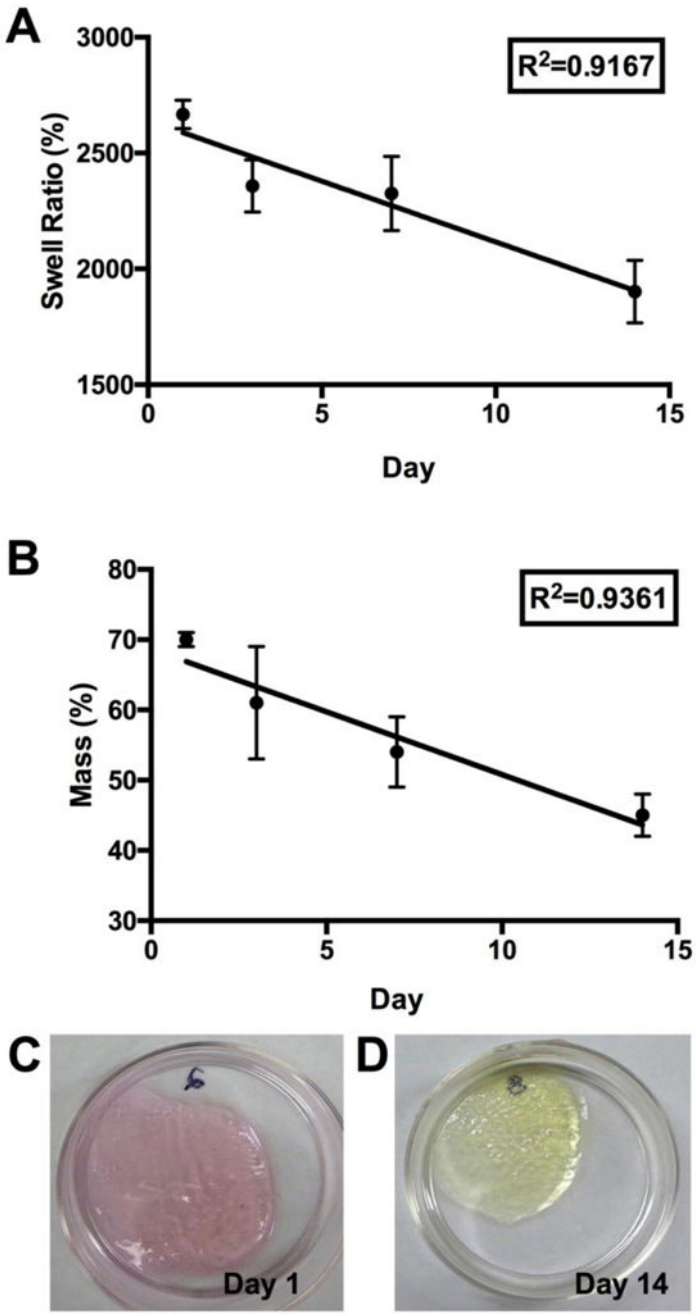

Figure 6.

The effects of degradation on swell ratio, mass loss, and course visual observation, were assessed using 6% (w/v) alginate-based sealant patches over a 14-day period at 37°C. (A) Swell ratios decreased dramatically over the 14-day period, due to the reduction in polymer content; (B) hydrogel sealant patch mass decreased by greater than 50% over the 14-day period. (C) Image of an alginate-based hydrogel sealant patch on Day 1. (D) After 14-days of degradation, visible pitting/surface-erosion was observed on the surface of the hydrogel.

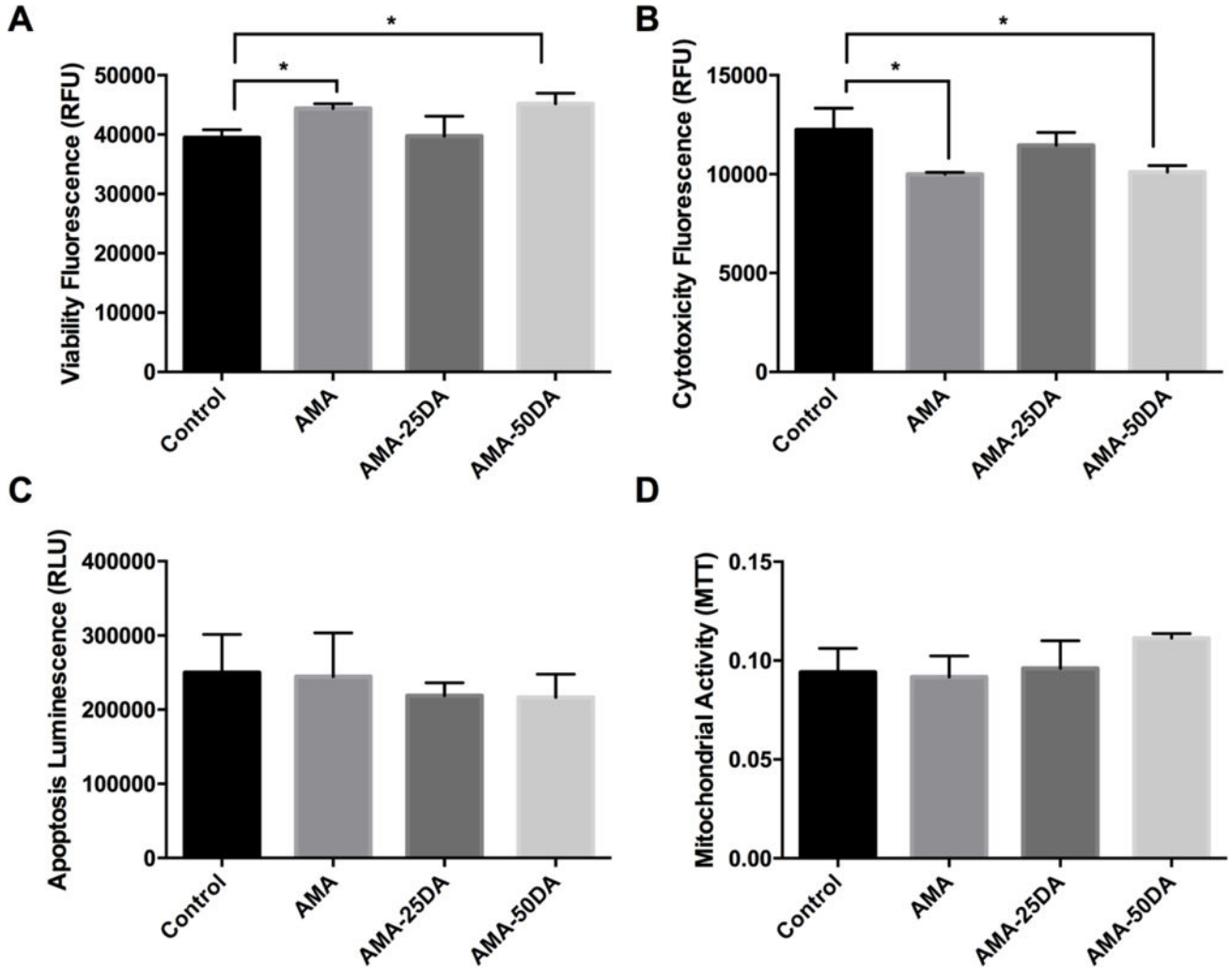

Figure 7.

(A) MeT-5A healthy human mesothelial cell viability, (B) cytotoxicity, (C) apoptosis and (D) mitochondrial activity after 24 hours of exposure to alginate-based sealant patch materials, as compared to non-treated control. Increases in overall cell viability were shown for AMA and AMA-25DA groups, as were decreased cytotoxicity, when compared to control. No significant differences in apoptosis and mitochondrial activity was observed.

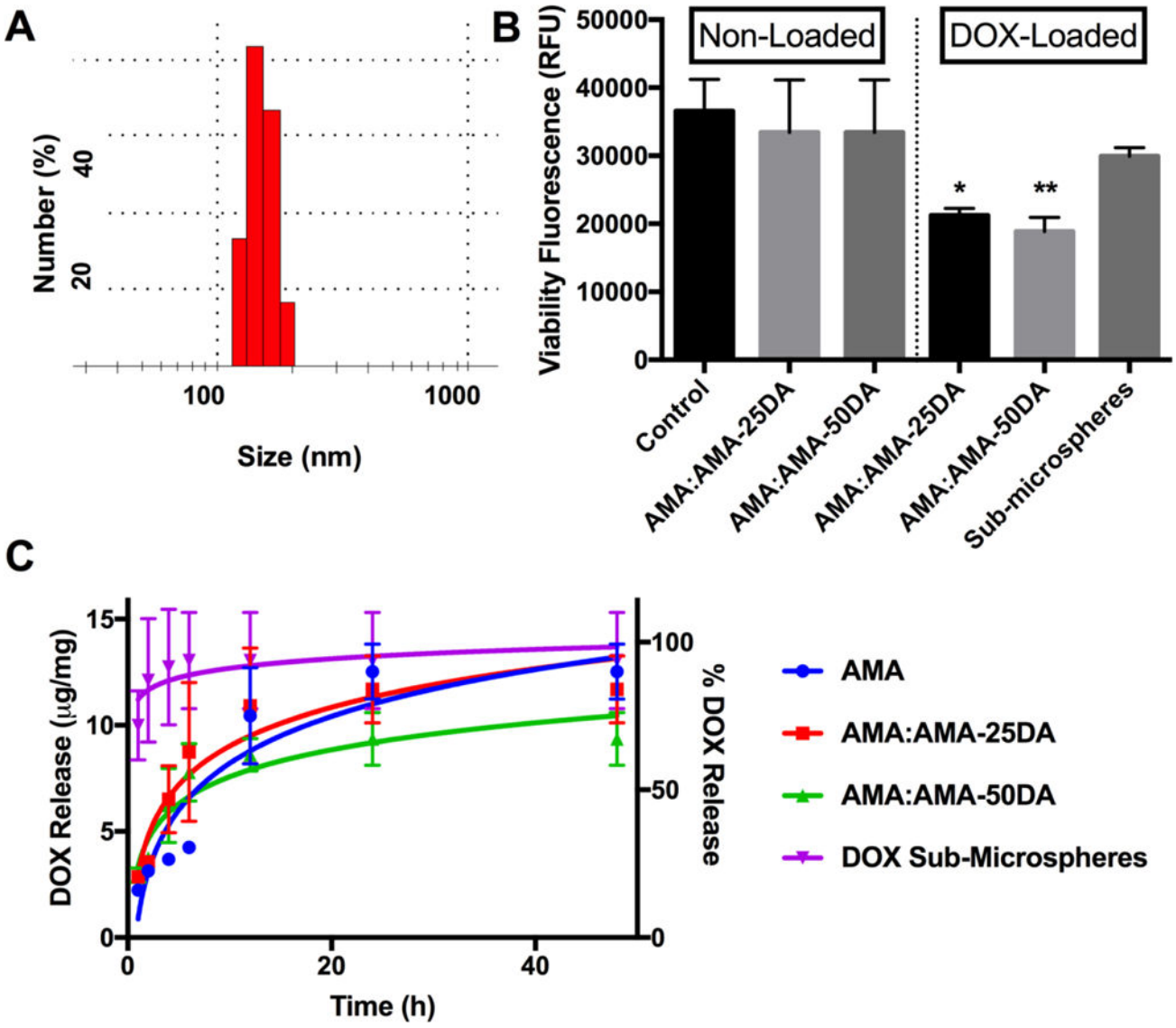

Figure 8.

(A) DOX-loaded AMA sub-microsphere number-average diameter distribution was quantified by DLS in PBS (pH 7.4) at 37°C; the average diameter was approximately 150 nm ± 19 nm. (B) A549 cell viability after 24 h exposure to non-loaded and DOX-loaded sealant patches and sub-microspheres. No significant differences in viability were detected between control and non-loaded sealant patches. Viability is however decreased significantly for both DOX-loaded patch formulations tested. DOX-loaded sub-microspheres did not exhibit a significant reduction in viability at p=0.05. (C) Drug release profiles (Left y-axis: micrograms DOX per milligram particles; Right y-axis: percentage of encapsulated DOX released) of DOX-loaded patches and sub-microspheres over 48 hours at 37°C.

Table 1

Summary of patch formulations tested, including polymer concentrations, blend ratios, degrees of methacrylation (DOM) and oxidation/aldehyde-modification (DOO), average burst pressures achieved prior to failure, and the mode of sealant failure (delamination/adhesive-failure is denoted by D, and material failure/rupture is denoted by M).

Polymer Group	Conc. (%, w/v)	AMA:AMA-DA Blend Ratio	DOM (%)	DOO (%)	Burst Pressure (in H_2O)	Mode of Failure
AMA	3	1:0	58	0	41.0 ± 23.7	D
AMA-25DA		1:1	48	10	7.7 ± 8.4	M
AMA-50DA			47	21	5.3 ± 6.6	M
AMA	4.5	1:0	58	0	51.8 ± 34.9	D
AMA-25DA		1:1	48	10	25.3 ± 5.8	M
AMA-50DA			47	21	5.9 ± 7.48	M
AMA-25DA		1:2	45	13	20.6 ± 13.8	M
AMA-50DA			43	28	12.0 ± 3.9	M
AMA-25DA		2:1	51	6	65.3 ± 50.3	D
AMA-50DA			51	14	77.3 ± 53.3	D
AMA	6	1:0	58	0	142.0 ± 34.5	D
AMA-25DA		1:1	48	10	200.8 ± 11.9	M
AMA-50DA			47	21	119.2 ± 21.6	M